NUMERICAL STUDY OF NATURAL TURBULENT CONVECTION OF NANOFLUIDS IN A TALL CAVITY HEATED FROM BELOW

by

Ridha MEBROUK [a,b,c*], Mahfoud KADJA [a], Mohamed LACHI[b], and Stephane FOHANNO[b]

[a] Laboratory of Applied Energetics and Pollution, Department of Mechanical Engineering, University Mentouri, Constantine, Algeria
[b] Laboratory of Thermo-Mechanics, GRESPI, University of Reims Champagne Ardenne, Reims, France
[c] Department of Hydrocarbon and Chemistry, University of Kasdi Merbah Ouargla, Ouargla, Algeria

Original scientific paper
DOI: 10.2298/TSCI150225089M

In the present paper a numerical study of natural turbulent convection in a tall cavity filled with nanofluids. The cavity has a heat source embedded on its bottom wall, while the left, right, and top walls of the cavity are maintained at a relatively low temperature. The working fluid is a water based nanofluid having three nanoparticle types: aluminum, Cu, and CuO. The influence of pertinent parameters such as Rayleigh number, the type of nanofluid, and solid volume fraction of nanoparticles on the cooling performance is studied. Steady forms of 2-D Reynolds-averaged-Navier-Stokes equations and conservation equations of mass and energy, coupled with the Boussinesq approximation, are solved by the control volume based discretisation method employing the SIMPLE algorithm for pressure-velocity coupling. Turbulence is modeled using the standard k-ε model. The Rayleigh number is varied from 2.4910^{09} to 2.4910^{11}. The volume fractions of nanoparticles were varied in the interval $0 \leq \varphi \leq 6\%$. Stream lines, isotherms, velocity profiles, and temperature profiles are presented for various combinations of Rayleigh number, the type of nanofluid, and solid volume fraction of nanoparticles. The results are reported in the form of average Nusselt number on the heated wall. It is shown that for all values of Rayleigh number, the average heat transfer rate from the heat source increases almost linearly, and monotonically as the solid volume fraction increases. Finally, the average heat transfer rate takes on values that decrease according to the ordering Cu, CuO, and Al_2O_3.

Key words: *nanofluid, turbulent flow, convection, bottom-heated enclosures, heat transfer*

Introduction

Natural convection in enclosures has many applications for example in building design (*i. e.* ventilation), in solar energy systems, in electronic equipment cooling, and in solar collectors [1]. In last ten years, many experimental and numerical studies of natural convection in enclosures configurations have been conducted. We can mention for example: Calcagni *et al.* [1] who have obtained experimental data by measuring the temperature distribution in the air layer by real time and double-exposure holographic interferometry. Corvaro and

* Corresponding author; e-mail: ridhamebrouk@gmail.com

Paroncini [2-4] have measured natural convection heat transfer in square cavities heated from below using particle image velocimetry (PIV) and holographic interferometry techniques. Heat transfer by convection can be enhanced passively by changing the geometry or the position of the boundary conditions, or by enhancing the thermal conductivity of the base fluid, for example, by adding small solid nanoparticles to form a nanofluid. So we have a new fluid that is called nanofluid. The nanofluids, Choi and Eastman [5], are colloidal solutions obtained by dispersing solid particles of nanometer size (10^{-9} m) in a base fluid. At very low concentrations, some of these solutions are proven to be very effective for enhancing heat transfer. Studies on nanofluids are numerous and diverse we can mention for example: Khanafer *et al*. [6] who were the first to investigate the problem of buoyancy-driven heat transfer enhancement of nanofluids. They used the finite-volume approach along with the alternating direct implicit procedure, to investigate numerically the natural convection heat transfer of a Cu-water nanofluid in a square enclosure differentially heated through the vertical side walls. The authors reported that the suspended nanoparticles substantially increase the heat transfer at any given Grashof number and that the nanofluid heat transfer rate increases with an increase in the nanoparticles volume fraction. Aminossadati and Ghasemi [7] reported the results of a numerical finite volume study of natural convection in a square enclosure heated from below and cooled through the top and vertical walls. They used nanofluids made with different types of nanoparticles (Cu, Ag, Al_2O_3, and TiO_2). They found that Cu and Ag nanoparticles have the highest cooling performance especially at low Rayleigh numbers, and even though, the addition of Al_2O_3 and TiO_2 also reduces the heat source maximum temperature, their influence is not as significant as that due to Cu and Ag nanoparticles. Oztop and Abu-Nada [8] used the finite element method to simulate heat transfer and fluid flow due to buoyancy forces in a partially heated enclosure using nanofluids with various types of nanoparticles. They found that the heat transfer enhancement, using nanofluids, is more pronounced at low aspect ratio than at high aspect ratio. Jahanshahi *et al.* [9] used experimental and theoretical values of thermal conductivity in a study of natural convection in a differentially heated square cavity. They reported the numerical results obtained using the finite volume approach. They concluded that the mean Nusselt number increases with volume fraction for the whole range of Rayleigh numbers. However, by using the theoretical formulations for conductivity no enhancement has been observed. Ho *et al.* [10] have investigated the effects due to uncertainties, in the various formulas of effective dynamic viscosity and thermal conductivity of aluminum-water nanofluid, on the heat transfer characteristics in a square vertical enclosure. They concluded that the uncertainties associated with different formulas adopted for the effective thermal conductivity and dynamic viscosity of the nanofluid have a strong bearing on the natural convection heat transfer characteristics in the enclosure. Santra *et al.* [11] used a Cu-water nanofluid to study the effects of Rayleigh number and volume fraction of nanoparticles on the heat transfer due to laminar natural convection in a differentially heated square cavity. Their results show that the heat transfer decreases with increase in volume fraction for a particular Rayleigh number, while it increases with Rayleigh number for a particular volume fraction. Aminossadati and Ghasemi [12] conducted a numerical study of natural convection in a 2-D square cavity filled with a CuO-water nanofluid. They used two pairs of heat source-sink to cover the entire length of the bottom wall of the cavity while the other walls are thermally insulated. Their results showed that regardless of the position of the pairs of source-sink the heat transfer rate increases with an increase of the Rayleigh number and the solid volume fraction. Guimaraes and Menon [13] have investigated numerically the effects of Rayleigh number, volume fraction of different nanoparticles, and fin height on the heat trans-

fer inside a square enclosure with a protuberant heat source that may resemble an electrical transformer. The authors reported that the nanofluids proved to smoothly enhance heat transfer as the concentration increases. They also concluded that nanoparticle materials play an important role on Nusselt number. The highest heat transfer values were obtained with Cu nanoparticles. Mahmoudi *et al.* [14] numerically studied natural convection cooling of a heat source horizontally attached to the left vertical wall of a cavity filled with a Cu-water nanofluid. The left vertical wall was kept at a constant temperature, while the other ones were kept adiabatic. Their results showed that the average Nusselt number decreases with an increase in the length of the heater and increases linearly with the increase in the solid volume fraction of the nanofluid. They also concluded that the increase of Rayleigh numbers strengthens the natural convection flows which leads to the decrease in heat source temperature. Jou and Tzeng [15] investigated the effects of Rayleigh number, aspect ratios and volume fraction of nanoparticles on heat transfer performance of nanofluids inside an enclosure. They used the Khanefer's model in their analyzis. They concluded that an increase of the buoyancy parameter and the volume fraction of nanofluids causes an increase in the average heat transfer coefficient. Rezaiguia *et al.* [16] conducted a numerical study of natural convection cooling of a heat source located on the bottom wall of an inclined isosceles triangular enclosure filled with a Cu-water nanofluid. They concluded that the existence of the nanoparticles increases the heat transfer for all Rayleigh number and a critical value for the inclination angle was determined for which the heat source maximum temperature is the highest. All their studies were conducted for the laminar regime of natural convection in enclosures.

The objective of our study is to investigate numerically heat transfer enhancement in a tall enclosure in which natural turbulent convection takes place with a nanofluid as the working fluid and with constant heat flux heating imposed on the bottom wall. The effects of volume fraction of the nanoparticles, Rayleigh number and type of nanofluids on the fluid flow and heat transfer inside the enclosure are presented.

Physical model and governing equations

The physical model, co-ordinate system and geometrical parameters corresponding to the configuration, are presented in fig. 1. It is a tall enclosure, its left, right, and top walls are kept cold at a constant temperature, T_c, while its bottom wall is kept hot with a constant heat flux, q''. The used fluid in the cavity is a water-based nanofluid containing nanoparticles.

The steady-state governing equations (mass, momentum, and energy) for the 2-D turbulent natural convection with the conservation equation for turbulent kinetic energy, k, and its dissipation rate, ε, are:

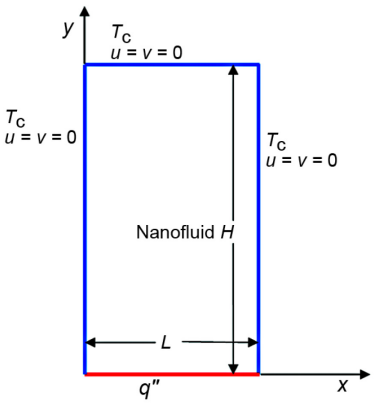

Figure 1. Schematic diagram of the physical domain and boundary conditions

$$\frac{\partial}{\partial x}(\rho_{nf}u)+\frac{\partial}{\partial y}(\rho_{nf}v)=0 \tag{1}$$

$$\frac{\partial}{\partial x}(\rho_{nf}uu)+\frac{\partial}{\partial y}(\rho_{nf}vu) = -\frac{\partial p}{\partial x}+\frac{\partial}{\partial x}\left[2(\mu_{eff})_{nf}\frac{\partial u}{\partial x}\right]+\frac{\partial}{\partial y}\left[(\mu_{eff})_{nf}\left(\frac{\partial u}{\partial y}+\frac{\partial v}{\partial x}\right)\right] \tag{2}$$

$$\frac{\partial}{\partial x}(\rho_{\mathrm{nf}} uv) + \frac{\partial}{\partial y}(\rho_{\mathrm{nf}} vv) = -\frac{\partial p}{\partial y} + \frac{\partial}{\partial x}\left[2(\mu_{\mathrm{eff}})_{\mathrm{nf}} \frac{\partial v}{\partial y}\right] +$$

$$+\frac{\partial}{\partial y}\left[(\mu_{\mathrm{eff}})_{\mathrm{nf}} \left(\frac{\partial v}{\partial x} + \frac{\partial u}{\partial y}\right)\right] + (\rho\beta)_{\mathrm{nf}} \mathrm{g}(T - T_0) \tag{3}$$

$$\frac{\partial}{\partial x}(\rho_{\mathrm{nf}} uc_p T) + \frac{\partial}{\partial y}(\rho_{\mathrm{nf}} vC_p T) = \frac{\partial}{\partial x}\left[(\lambda_{\mathrm{eff}})_{\mathrm{nf}} \frac{\partial T}{\partial x}\right] + \frac{\partial}{\partial y}\left[(\lambda_{\mathrm{eff}})_{\mathrm{nf}} \frac{\partial T}{\partial y}\right] \tag{4}$$

$$\frac{\partial}{\partial x}(\rho_{\mathrm{nf}} uk) + \frac{\partial}{\partial y}(\rho_{\mathrm{nf}} vk) = \frac{\partial}{\partial x}\left[\left(\mu + \frac{\mu_t}{\sigma_k}\right)_{\mathrm{nf}} \frac{\partial k}{\partial x}\right] + \frac{\partial}{\partial y}\left[\left(\mu + \frac{\mu_t}{\sigma_k}\right)_{\mathrm{nf}} \frac{\partial k}{\partial y}\right] + P_{\mathrm{k}} + G_{\mathrm{k}} - \rho_{\mathrm{nf}}\varepsilon \tag{5}$$

$$\frac{\partial}{\partial x}(\rho_{\mathrm{nf}} u\varepsilon) + \frac{\partial}{\partial y}(\rho_{\mathrm{nf}} v\varepsilon) = \frac{\partial}{\partial x}\left[\left(\mu + \frac{\mu_t}{\sigma_\varepsilon}\right)_{\mathrm{nf}} \frac{\partial \varepsilon}{\partial x}\right] + \frac{\partial}{\partial y}\left[\left(\mu + \frac{\mu_t}{\sigma_\varepsilon}\right)_{\mathrm{nf}} \frac{\partial \varepsilon}{\partial y}\right] +$$

$$+[C_{\varepsilon 1}(P_k + C_{\varepsilon 3} G_k) - C_{\varepsilon 2}\varepsilon]\frac{\varepsilon}{k} \tag{6}$$

where

$$P_{\mathrm{k}} = (\mu_t)_{\mathrm{nf}}\left[2\left(\frac{\partial u}{\partial x}\right)^2 + 2\left(\frac{\partial v}{\partial y}\right)^2 + \left(\frac{\partial u}{\partial y} + \frac{\partial v}{\partial x}\right)^2\right], \qquad G_{\mathrm{k}} = -\frac{(\mu_t)_{\mathrm{nf}}}{\sigma_T}\mathrm{g}\beta_{\mathrm{nf}}\frac{\partial T}{\partial y},$$

$$(\mu_{\mathrm{eff}})_{\mathrm{nf}} = \mu_{\mathrm{nf}} + (\mu_t)_{\mathrm{nf}}, \qquad (\mu_t)_{\mathrm{nf}} = C_\mu \frac{\rho_{\mathrm{nf}} k^2}{\varepsilon}, \qquad \text{and} \qquad (\lambda_{\mathrm{eff}})_{\mathrm{nf}} = \lambda_{\mathrm{nf}} + \frac{(\mu_t)_{\mathrm{nf}} c_{p_{\mathrm{nf}}}}{\sigma_T}$$

where the coefficients of the *k*-ε model have the following standard values [17]:

$$C_\mu = 0.09, \quad C_{\varepsilon 1} = 1.44, \quad C_{\varepsilon 2} = 1.44, \quad C_{\varepsilon 3} = \tanh\left(\frac{v}{u}\right), \quad \sigma_T = 1.0, \quad \sigma_k = 1.0, \quad \sigma_\varepsilon = 1.3$$

The boundary conditions, used to solve eqs. (1)-(6):
On the right, left, and top walls we have:

$$u = v = \varepsilon = k = 0, \qquad T = T_{\mathrm{c}}$$

On the bottom wall the boundary conditions are:

$$u = v = \varepsilon = k = 0, \qquad -\lambda\frac{\partial T}{\partial y} = q''$$

The effective density, thermal diffusivity, heat capacitance, and thermal expansion coefficient of the nanofluid are calculated using the following expressions:

$$\rho_{\mathrm{nf}} = (1-\varphi)\rho_{\mathrm{f}} + \varphi\rho_{\mathrm{s}} \tag{7}$$

$$(\rho c_p)_{\mathrm{nf}} = (1-\varphi)(\rho c_p)_{\mathrm{f}} + \varphi(\rho c_p)_{\mathrm{s}} \tag{8}$$

$$(\rho\beta)_{\mathrm{nf}} = (1-\varphi)(\rho\beta)_{\mathrm{f}} + \varphi(\rho\beta)_{\mathrm{s}} \tag{9}$$

$$\alpha_{\mathrm{nf}} = \frac{\lambda_{\mathrm{nf}}}{(\rho c_p)_{\mathrm{nf}}} \tag{10}$$

where φ is the solid volume fraction. The effective dynamic viscosity of the nanofluid is calculated using the formula suggested by Brinkman [16]:

$$\mu_{\mathrm{nf}} = \frac{\mu_{\mathrm{f}}}{(1-\varphi)^{2.5}} \tag{11}$$

The effective thermal conductivity of the nanofluid is approximated by the Maxwell-Garnetts model, for a suspension of spherical nanoparticles in a base fluid, the formula is [16]:

$$K_{\mathrm{nf}} = K_{\mathrm{f}}\left[\frac{(K_{\mathrm{s}} + 2K_{\mathrm{f}}) - 2\varphi(K_{\mathrm{f}} - K_{\mathrm{s}})}{(K_{\mathrm{s}} + 2K_{\mathrm{f}}) + \varphi(K_{\mathrm{f}} - K_{\mathrm{s}})}\right]$$

The thermo-physical properties of the base fluid and the nanoparticles (at 293 K) are presented in tab. 1.

Table 1. Thermo-physical properties of the base fluid and the nanoparticles [18]

Properties	Pure water	Cu	CuO	Al_2O_3
c_p [$Jkg^{-1}K^{-1}$]	4181.8	385	561	761.55
ρ [kgm^{-3}]	998.2	8954	6450	3960.14
λ [$Wm^{-1}K^{-1}$]	0.593	401	20	37.17
β [K^{-1}]·10^5	2.1	1.67	1.8	0.75

One can calculate the local heat transfer coefficient, h_x, through the bottom wall using this formula:

$$h_x = \frac{q''}{T_{\mathrm{s}}(x) - T_{\mathrm{c}}} \tag{12}$$

where $T_{\mathrm{s}}(x)$ is the local temperature on the heated surface. This value of h_x is used to calculate the local Nusselt number given by:

$$\mathrm{Nu}_{\mathrm{s}} = \frac{h_x L}{K_{\mathrm{f}}} \tag{13}$$

The average Nusselt number, is determined by integrating Nu_{s} along the active part of the hot wall [16]:

$$\mathrm{Nu} = \frac{\overline{h}L}{K_{\mathrm{f}}} = \frac{1}{L}\int_0^L \mathrm{Nu}_x \,\mathrm{d}x \tag{14}$$

Numerical technique and validation

In this study, the dimensionless governing eqs. (1)-(6) with their boundary conditions are solved using the commercial software FLUENT (version 6.3). The SIMPLE algorithm is used to determine the pressure field, while the QUICK scheme is used to discretize the convection terms in the momentum and energy equations. Turbulence is modeled by using the standard k-ε model. The Gambit code is used to generate the grid of the simulated domain. The grid system for the computational domain is created using unstructured quadrilateral cells. In order to obtain a grid independent solution, a grid refinement study is performed for the enclosure with the following parameter values: $A = 4$, $Ra = 2{,}5 \cdot 10^{10}$, and $\varphi = 0$ (pure water).

Table 2. Results of the grid independence study for Ra =2,5·10^{10} and $\varphi = 0$

Simul. No.	Grid size	Average Nu	% Change
1	30 × 60	22.581	–
2	40 × 60	22.606	0.111
3	50 × 60	22.607	0.004

Table 3. Validation of the numerical results in terms of average Nusselt number

	$Ra = 10^3$ $\overline{Nu}$	$Ra = 10^4$ $\overline{Nu}$	$Ra = 10^5$ $\overline{Nu}$
Present	1.100	2.217	4.498
Khanafer *et al.* [6]	1.114	2.245	4.510
Barakos and Mistoulis [19]	1.108	2.201	4.430

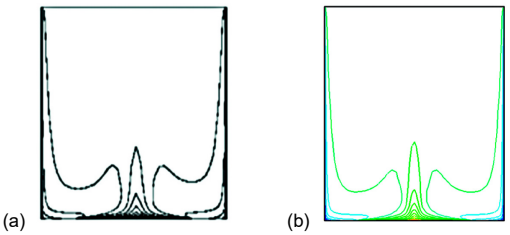

Figure 2. Isotherms for Ra = 10^{10}; (a) numerical results in [17], (b) present numerical results

The mean Nusselt number obtained using different grid numbers for the previous case is presented in tab. 2. The relative errors reach an asymptotic value of 0.004 indicating that a 50 × 60 uniform grid can be used with acceptable precision in the computed results.

In order to validate our study at low Rayleigh number, the results were compared to those obtained by Khanafer *et al.* [6] and Barakos and Mistoulis [19] with similar boundary conditions and in the laminar regime. Table 3 presents this comparison. The difference between the average Nusselt number of Khanafer *et al.* [6] and Barakos and Mistoulis [19], and that obtained by the present simulations is well within acceptable limits and gives confidence in the numerical results to be reported subsequently.

To validate our numerical simulation at high Rayleigh numere by comparing our results with those published by Sharma *et al.* [17] (the fluid used is air in a square cavity of dimensions with a localized heat source at the center of the lower horizontal wall in these simulations, we used the same Rayleigh number and the same length of the heated portion than [17] (which is the ratio between the length of the heat source with respect to the total length of the lower horizontal wall). Sharma *et al.* [17] have obtained their numerical results using the FLUENT code.

Figure 2 shows that there is a very good qualitative agreement and a good quantitative agreement between the results obtained in this work and those obtained in [17], which is used to validate our numerical simulation procedure.

Table 4 presents the difference between the average Nusselt number of [17] and that obtained by the present simulations is well within acceptable limits and gives confidence in the numerical results to be reported subsequently.

Table 4. Validation of the numerical results in terms of average Nusselt number at high Rayleigh number

	$Ra = 10^9$ $\overline{Nu}$	$Ra = 10^{10}$ $\overline{Nu}$	$Ra = 10^{11}$ $\overline{Nu}$
Present	46.84	80.10	136.94
Sharma *et al.* [17]	47.00	80.38	137.44

Based on a parametric study [17], a correlation for the heat transfer rate has been proposed, to predict the heat transfer from the bottom wall of the enclosure. For the isothermal heating condition:

$$\overline{Nu} = 0.13\delta^{8}\, Ra^{0.334}$$

where δ is non-dimensional heated width.

Results and discussion

In this numerical study, the overall objective is to explore the heat transfer behavior of natural turbulent convection inside a tall cavity with Cu-water, CuO-water, and Al_2O_3-water nanofluides. Analysis of the results is made through obtained isotherms, streamlines, mid-height vertical velocities and temperature, average Nusselt number, for the previous types of nanofluids, and for the two important parameters, φ and Ra. The ranges are varied as $0 \le \varphi \le 6\%$ and $2.5\cdot10^9 \le Ra \le 2.5\cdot10^{11}$. The value $\varphi = 0$, corresponds to the case where the working fluid is pure water (zero content of nanoparticles).

Figure 3 shows the influence of the volume fraction, φ, on the distribution of vertical velocity, v, for $Ra = 2.4910^{10}$, at the horizontal mid-plane ($y = H/2$) of the vertical cavity for different nanofluids. This figure shows clearly a wavy and symmetrical v-velocity profile. It is observed that when nanoparticles are added the thickness of the slow moving fluid layer at the left and right walls of the cavity decreases with the increase in φ. This happens as a result of increase in momentum transport through the fluid. This increase in momentum transport is due to the high velocities which result from the enhanced convection. The same remarks apply to all types of nanofluids and one can notice that the difference between the thicknesses of the two layers is highest for Cu, and lowest for Al_2O_3, This phenomenon is also observed by other researchers in this type of convective exchanges [20, 21].

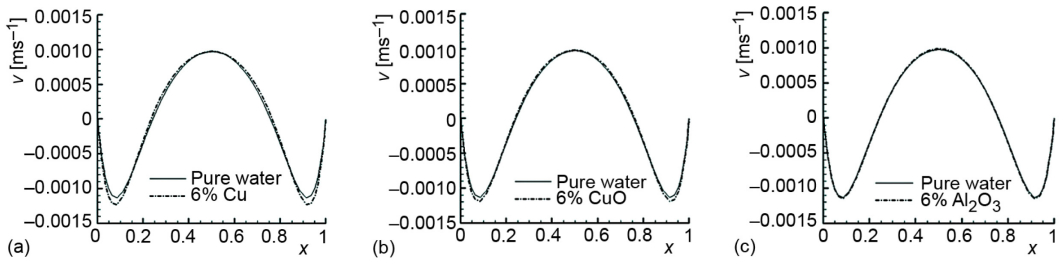

Figure 3. Vertical velocity profile at mid plane for different φ values for $Ra = 2.5\cdot10^{10}$; (a) Cu-water, (b) CuO-water, and (c) Al_2O_3-water

Figure 4 shows the v velocity component distribution in the mid-plane of the cavity. The fluid being heated at the bottom wall of the cavity (corresponding to $Y = 0$) moves to the top wall with a velocity influenced by the type of nanofluid. We can also notice that the addition of Cu nanoparticles in the base fluid (pure water) gives rise to the highest upward flow intensity as compared to CuO and Al_2O_3. The addition of Al_2O_3 particles has the least influence on the upward flow intensity.

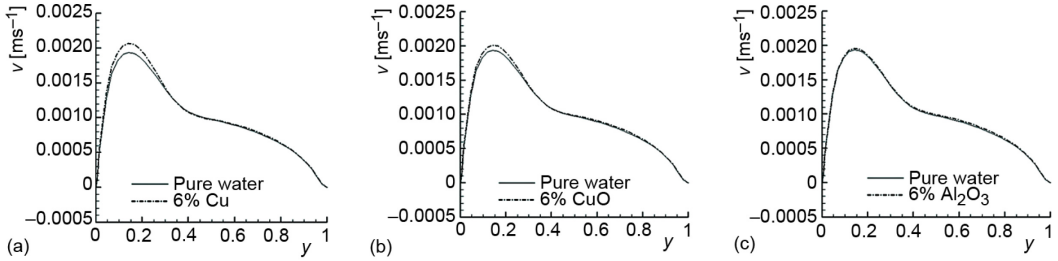

Figure 4. Vertical velocity profile at mid plane for different φ values for Ra = $2.5 \cdot 10^{10}$; (a) Cu-water, (b) CuO-water, and (c) Al_2O_3-water

The effects of Rayleigh number on the distribution of vertical velocity component v for $\varphi = 6\%$, at the horizontal mid-plane $(y = H/2)$ of the vertical cavity for different nanofluids are shown in fig 5. One can notice from this figure a wavy and symmetrical form of the velocity profile. The thickness of the slow moving fluid layer at the left and right walls of cavity decreases with the increase in Rayleigh number for all different nanofluids. One can also notice that when the Rayleigh number increases the absolute maximum value in the profile of the v velocity component increases. This is due to the fact that the buoyant force is increased with increasing Rayleigh number. Also, increasing Rayleigh number enhances the mixing within the boundary layers due to the increase of turbulence and therefore the eddy viscosity responsible for momentum diffusion. Heat transfer performance by natural convection is therefore enhanced due to the decrease of the thermal resistance of boundary layers in contact with the cavity walls.

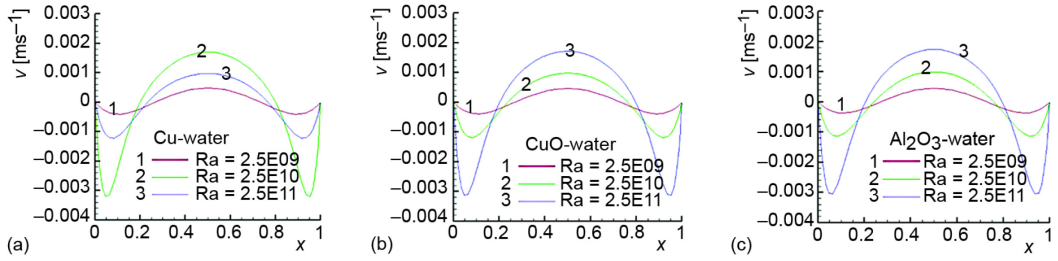

Figure 5. Vertical velocity profile at mid-plane for different Rayleigh number with φ = 6%; (a) Cu-water, (b) CuO-water, and (c) Al_2O_3-water

Figure 6 shows the temperature profile at the mid plane ($Y = 0.5$) for different φ values for Ra = $2.49 \cdot 10^{10}$. When the nanoparticles are added (*i. e.* increase in φ value), it is clearly seen that the fluid temperature decreases across the mid-plane, for all the different types of nanofluids. From fig. 7 it is clear that this decrease in temperature is highest for Cu, and smallest for Al_2O_3. The values corresponding to CuO are situated in between. The decrease in temperature difference is an indication of enhanced fluid cooling *i. e.* increased rate of heat transfer between the fluid and the surrounding ambient medium.

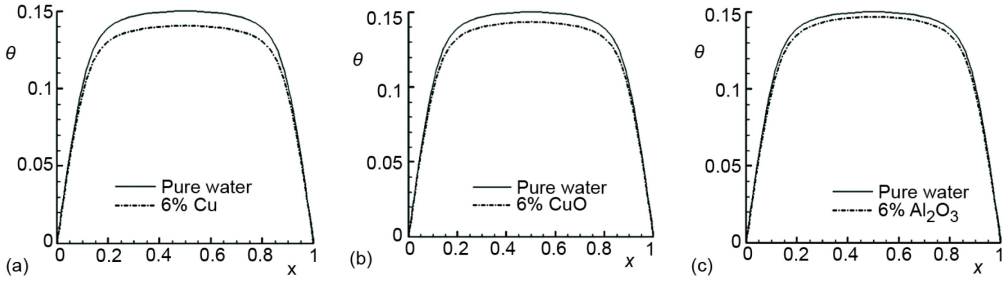

Figure 6. Temperature profile at mid-plane for different φ values for Ra = $2.49 \cdot 10^{10}$

Rayleigh number and volume fraction of nanoparticles are key parameters for studying the effects of nanoparticles and buoyancy force on flow fields, temperature distributions, and rate of heat transfer. These effects can be clearly seen in figs. 8-10 which show streamlines (on the left) and isotherms (on the right) for three values of the Ra = $2.49 \cdot 10^{9}$, Ra = $2.49 \cdot 10^{10}$, and Ra = $2.49 \cdot 10^{11}$.

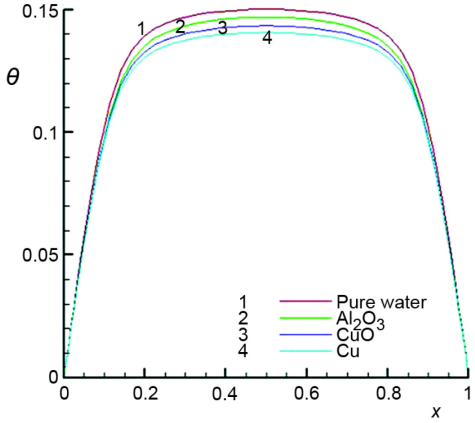

Figure 7. Temperature profile at mid-plane for different nanofluides, for Ra = $2.5 \cdot 10^{10}$ and φ = 6%

From the streamline contours one can notice the formation of two counter-rotating cells, the right hand cell rotates clockwise while the left hand cell rotates in the opposite direction. This observation is valid for all values of Rayleigh number and volume fraction [23, 24]. The fluid which is being heated through the bottom wall moves towards the upper cold wall and impinges on it [25]. The fluid jet then splits into two fluxes, one of which goes towards the left cold wall and the other goes towards the right cold wall. The two cells are nearly equal. We can also notice that as we increase the Rayleigh number, flow re-circulation inside the enclosure becomes more intense (because the streamlines become nearer to each other) and the center of the re-circulation zones moves upwards. The thickness of the thermal boundary layer

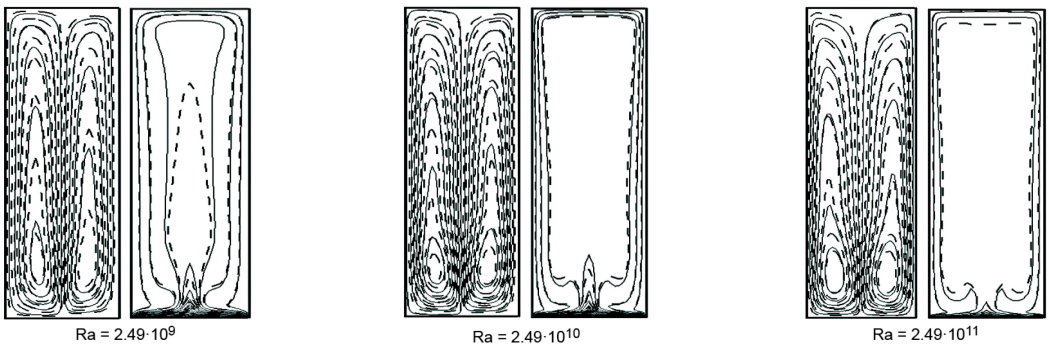

Figure 8. Streamlines and isotherms (Cu-water), (dashed line) at φ = 6% for different Rayleigh number

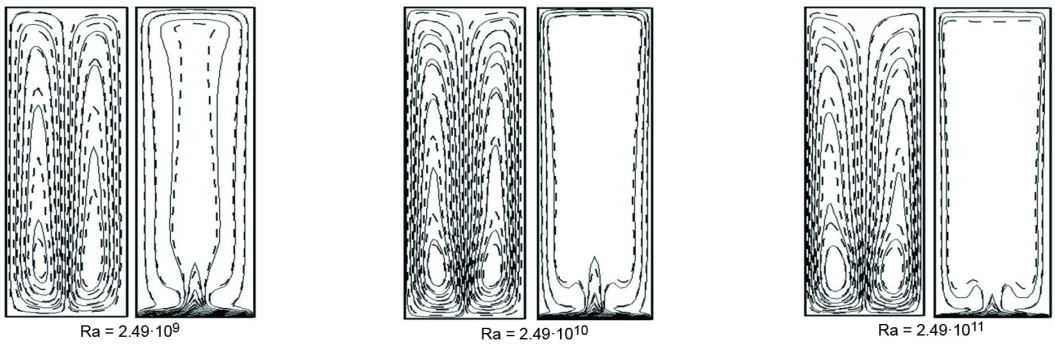

Figure 9. Streamlines and isotherms (Cu-water), (dashed line) at φ = 6% for different Rayleigh number

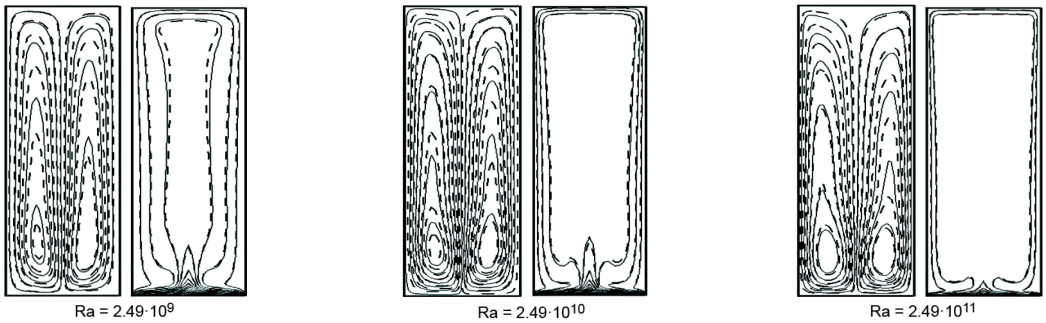

Figure 10. Streamlines and isotherms (water-Al_2O_3), (dashed line) at φ = 6% for different Rayleigh number

adjacent to the heated wall is influenced by the addition of nanoparticles (see isotherms in fig. 8 and the stratification of the isotherms breaks down with an increase in the volume fraction for higher Rayleigh number. This sensibility of the thermal boundary layer thickness to the volume fraction of nanoparticles is related to the increased viscosity and thermal conductivity at high volume fraction of nanoparticles. If we compare the isotherms as a function of Rayleigh number, we can notice that, as Rayleigh number increases, the isotherms become nearer to each other in the region situated in the proximity of the bottom wall [24], *i. e.* the heated wall. This implies that temperature gradients become higher close to the bottom wall, *i. e.* that the heat fluxes through the bottom wall increase as Rayleigh number increases. We can observe clearly from the isotherm contours that the highest temperatures are those of the fluid which circulates near the heated wall [26], and that the lowest temperatures are those of the fluid which circulates near the cold walls.

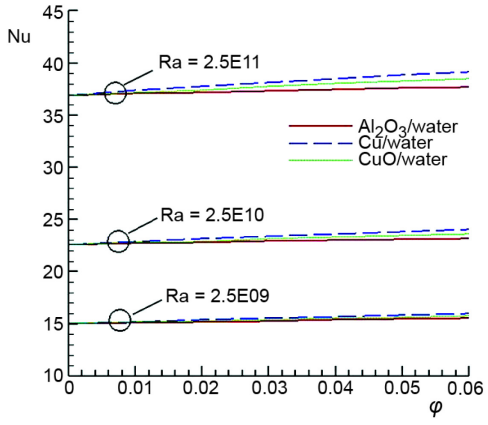

Figure 11. Variation of mean Nusselt numbers with solid volume fraction at different values of Rayleigh numbers for different nanofluids; (a) Cu-water, (b) CuO-water, (c) water-Al_2O_3

Therefore, the fluid heats up in contact with the heated region and cools down in contact with the cold walls [27].

The heat transfer rate is characterized by the average Nusselt number calculated along the region of the bottom wall. Figure 11 illustrates the variation of average Nusselt number as a function of the solid volume fraction of nanofluid φ and the Rayleigh number. For all values of Rayleigh number, the average Nusselt number increases almost linearly as the solid volume fraction increases [28] from 0% (pure water) to 6%. This enhancement in heat transfer is due to the increase in the nanofluid effective thermal conductivity, which in turn is due to the increase of the nanoparticles in the base fluid.

Figure 12 shows the variation of mean Nusselt numbers with solid volume fraction for different nanoparticles at Ra = $2.49 \cdot 10^{11}$. One can easily notice from the three curves that the average heat transfer rate takes on values that decrease according to the ordering Cu, CuO, and Al_2O_3. The lowest heat transfer was obtained for Al_2O_3 due to the decrease of conduction mode heat transfer, since Al_2O_3 has the lowest value of the thermal conductivity compared to Cu and CuO.

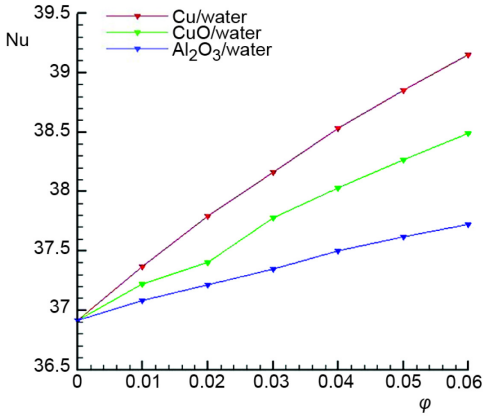

Figure 12. Variation of mean Nusselt numbers with solid volume fraction for different nanoparticles at Ra = $2.49 \cdot 10^{11}$

Figure 11 also show that at low values of Rayleigh number ($2.49 \cdot 10^9$) the increase in φ is more influential on mean Nusselt number than at high values of Rayleigh number.

Three correlations for Cu-water, CuO--water, and Al_2O_3-water have been developed using least squares regression for the isoflux heating condition, to predict the heat transfer from the bottom wall of the enclosure, in terms of Rayleigh number ($2.49100^9 \leq$ Ra $\leq$ Ra = $2.49 \cdot 10^{11}$) and the particles volume fraction ($0.01 \leq \varphi \leq 0.06$). Using the results from the present simulations, the three correlations can be expressed:

– for Cu-water:

$$\mathrm{Nu} = 0.2487\varphi^{0.0266}\,\mathrm{Ra}^{0.1950}$$

and the data agree to within ±1.75% of those predicted by the previous correlation;

– for CuO-water

$$\mathrm{Nu} = 0.2487\varphi^{0.0204}\,\mathrm{Ra}^{0.1946}$$

and the data agree to within ±2.34% of those predicted by the previous correlation;

– for Al_2O_3-water

$$\mathrm{Nu} = 0.2487\varphi^{0.0120}\,\mathrm{Ra}^{0.1937}$$

and the data agree to within ±4.28% of those predicted by the previous correlation.

In other words, as one increases the Cu nanoparticles concentration in water, the percentage of heat transfer enhancement decreases as the Rayleigh number increases, for ex-

ample: a 6% increase of Cu nanoparticles concentration, increases the Nusselt number about 5.85 % at Ra = $2.49 \cdot 10^9$ and about 5.71% at Ra = $2.49 \cdot 10^{11}$. Although this increase in the average Nusselt number is small it plays a significant role in engineering applications such as in heating of buildings.

Conclusions

In this study we investigated numerically the heat transfer by natural turbulent convection in a cavity in order to show the enhancement of heat transfer due to the use of nanofluids as compared to the use of pure fluids. The parameters investigated are the type of nanofluid, the solid volume fraction, as well as the Rayleigh number. The results clearly show that the use of the nanofluids may considerably influence and enhance the heat transfer by using nanoparticles in this geometry. The principal conclusions obtained are:

- An increase in Rayleigh number gives rise to increased flow velocities and therefore to better heat removal because the buoyancy forces are increased.
- For all values of Rayleigh number, the average heat transfer rate from the heat source increases almost linearly and monotonically as the solid volume fraction increases.
- The average heat transfer rate takes on values that decrease according to the ordering Cu, CuO, and Al_2O_3.

This study and the results available in the literature indicate that the study of heat transfer of nanofluids is very complex and that there are many other factors that can influence the performance of nanofluids used for enhancing the heat transfer by natural convection.

Nomenclature

A – aspect ratio, [H/L]
C_u, $C_{\varepsilon 1}$, $C_{\varepsilon 2}$, $C_{\varepsilon 3}$ – constants of the turbulence model
G_k – buoyancy production/destruction of kinetic energy
c_p – specific heat, [Jkg^{-1}K^{-1}]
g – gravitational acceleration, [ms^{-2}]
H – height of the cavity, [m]
k – turbulent kinetic energy, [m^{2}s^{-2}]
Nu – Nusselt number along the heat source
P_k – production of turbulent kinetic energy
Pr – Prandtl number (θ_f/α_f)
p – fluid pressure, [Pa]
q'' – heat flux per unit area, [Wm^{-2}]
Ra – Rayleigh number [= $g\beta H^5 q''/(Lv\alpha)$]
T – temperature, [K]
ΔT – ref. temperature difference (= $q''L/k_f$), [K]
u, v – velocity components in x- and y-directions, [ms^{-1}]
x, y – cartesian coordinates, [m]
X, Y – dimensionless co-ordinates (x/H, y/H)

Greek symbols

α – thermal diffusivity, [m^{2}s^{-1}]
β – thermal expansion coefficient, [K^{-1}]
ε – dissipation rate of turbulent kinetic energy, [m^{2}s^{-3}]
θ – dimensionless temperature [= $(T - T_c/\Delta T$]
λ – thermal conductivity, [Wm^{-1}K^{-1}]
ε – dissipation rate of turbulent kinetic energy, [m^{2}s^{-3}]
μ – dynamic viscosity, [Nsm^{-2}]
ν – kinematic viscosity, [m^{2}s^{-1}]
ρ – density, [kgm^{-3}]
σ_k, σ_T, σ_ε, – turbulent Prandtl numbers of k, T, and ε
φ – solid volume fraction

Subscripts

c – cold wall
f – pure fluid
nf – nanofluids

References

[1] Calcagni, B. *et al.,* Natural Convective Heat Transfer in Square Enclosures Heated from Below, *Applied Thermal Engineering, 25* (2005), 16, pp. 2522-2531
[2] Corvaro, F., Paroncini, M., Experimental Analysis of Natural Convection in Square Cavities Heated from below with 2D-PIV and Holographic Interferometry Techniques, *Experimental Thermal and Fluid Science, 31* (2007), 7, pp. 721-739

[3] Corvaro, F., Paroncini, M., A Numerical and Experimental Analysis on the Natural Convective Heat Transfer of a Small Heating Strip Located on the Floor of a Square Cavity, *Applied Thermal Engineering, 28* (2008), 1, pp. 25-35
[4] Corvaro, F., Paroncini, M., An Experimental Study of Natural Convection in a Differentially Heated Cavity through a 2D-PIV System, *International Journal of Heat and Mass Transfer, 52* (2009), 1, pp. 355-365
[5] Choi, S. U. S., Eastman, J. A., Enhancing Thermal Conductivity of Fluids with Nanoparticles, *Proceedings,* ASME International Mechanical Engineering Congress & Exposition, San Francisco, Cal., USA, 1995
[6] Khanafer, K., *et al.,* Buoyancy-Driven Heat Transfer Enhancement in a Two-Dimensional Enclosure Utilizing Nanofluids, *International Journal of Heat and Mass Transfer, 46* (2003), 19, pp. 3639-3653
[7] Aminossadati, S. M., Ghasemi, B., Natural Convection Cooling of a Localised Heat Source at the Bottom of a Nanofluid-Filled Enclosure, *European Journal of Mechanics B/Fluids, 28* (2009), 5, pp. 630-640
[8] Oztop, H. F., Abu-Nada, E., Numerical Study of Natural Convection in Partially Heated Rectangular Enclosures Filled with Nanofluids, *International Journal of Heat and Fluid Flow, 29* (2008), 5, pp. 1326-1336
[9] Jahanshahi, M., *et al.,* Numerical Simulation of Free Convection Based on Experimental Measured Conductivity in a Square Cavity Using Water/SiO_2 Nanofluid, *International Communications in Heat and Mass Transfer, 37* (2010), 6, pp. 687-694
[10] Ho, C. J., *et al.,* Numerical Simulation of Natural Convection of Nanofluid in a Square Enclosure: Effects due to Uncertainties of Viscosity and Thermal Conductivity. *International Journal of Heat and Mass Transfer, 51* (2008), 17, pp. 4506-4516
[11] Santra, A. K., *et al.,* Study of Heat Transfer Augmentation in a Differentially Heated Square Cavity Using Copper-Water Nanofluid, *International Journal of Thermal Sciences, 47* (2008), 9, pp. 1113-1122
[12] Aminossadati, S. M., Ghasemi, B., Natural Convection of CuO-water Nanofluid in a Cavity with Two Pairs of Heat Source-Sink, *International Communications in Heat and Mass Transfer, 38* (2011), 5, pp. 672-678
[13] Guimaraes, P. M., Menon, G. J., Natural Nanofluid-Based Cooling of a Protuberant Heat Source in a Partially-Cooled Enclosure, *International Communications in Heat and Mass Transfer, 45* (2013), 1, pp. 23-31
[14] Mahmoudi, A. H., *et al.,* Numerical Study of Natural Convection Cooling of Horizontal Heat Source Mounted in a Square Cavity Filled with Nanofluid, *International Communications in Heat and Mass Transfer, 37* (2010), 8, pp. 1135-1141
[15] Jou, R.-Y., Tzeng, S.-C., Numerical Research of Nature Convective Heat Transfer Enhancement Filled with Nanofluids in Rectangular Enclosures, *International Communications in Heat and Mass Transfer, 33* (2006), 6, pp. 727-736
[16] Rezaiguia, I., *et al.* Numerical Computation of Natural Convection in an Isosceles Triangular Cavity with a Partially Active Base and Filled with a Cu-Water Nanofluid, *Heat Mass Transfer, 49* (2013), 9, pp. 1319-1331
[17] Sharma, A. K., *et al.,* Turbulent Natural Convection in an Enclosure with Localized Heating from Below, *International Journal of Thermal Sciences, 46* (2007), 12, pp. 1232-1241
[18] Bachir, G., Contribution to the Study of Natural Convection in Nanofluids in Rayleigh-Benard Configuration. Ph. D. thesis, University of Toulouse III, Paul Sabatier, Toulouse, France, 2010
[19] Barakos, G., Mistoulis, E., Natural Convection Flow in a Square Cavity Revisited: Laminar and Turbulent Models with Wall Functions, *Int. J. Numer. Meth. Heat Fluid Flow, 18* (1994), 7, pp. 695-719
[20] Pourmahmoud, N., *et al.*, Numerical Study of Mixed Convection Heat Transfer in Lid-Driven Cavity Utilizing Nanofluid: Effect of Type and Model of Nanofluid, *Thermal Science, 20* (2016), 1, pp. 347-358
[21] Oueslati, F. S., Bennacer, R., Heterogeneous Nanofluids: Natural Convection Heat Transfer Enhancement, *Nanoscale Research Letters, 6* (2011), 1, pp. 222-232
[22] Ternik, P., Rudolf, R., Conduction and Convection Heat Transfer Characteristics of Water-Based Au Nanofluids in a Square Cavity with Differentially Heated Side Walls Subjected to Constant Temperatures, *Thermal Science, 18* (2014), Suppl. 1, pp. S189-S200
[23] Cho, C.-C., *et al.,* Enhancement of Natural Convection Heat Transfer in a U-Shaped Cavity Filled with Al_2O_3 Water Nanofluid, *Thermal Science*, *16*, (2012), 5, pp. 1317-1323

[24] Mahmoodi, M., *et al.,* (2014). Free Convection of a Nanofluid in a Square Cavity with a Heat Source on the Bottom Wall and Partially Cooled from Sides, *Thermal Science, 18*, (2012), Suppl. 2, pp. S283-S300
[25] Chen., C.-L., *et al.,* Experimental and Numerical Studies on Periodic Convection flow and Heat Transfer in a Lid-Driven Arc-Shape Cavity, *International Communications in Heat and Mass Transfer, 39* (2012), 10, pp. 1563-1571
[26] Hakan, F., *et al.,* Experimental and Numerical Analysis of Buoyancy-Induced Fow in Inclined Triangular Enclosures, *International Communications in Heat and Mass Transfer, 39* (2012), 8, 1237-1244
[27] Sajjadi, H., Kefayati, R., Lattice Boltzmann Simulation of Turbulent Natural Convection in Tall Enclosures, *Thermal Science, 19* (2015), 1, pp. 155-166
[28] Sajadi, A. R., *et al.,* Experimental Study on Turbulent Heat Transfer, Pressure Drop, and Thermal Performance of ZnO/Water Nanofluid Flow in a Circular Tube, *Thermal Science, 18* (2014), 4, pp. 1315-1326

Paper submitted: February 25, 2015
Paper revised: December 20, 2015
Paper accepted: December 28, 2015